The Plant Cell, Vol. 8, 1391–1407, August 1996 © 1996 American Society of Plant Physiologists

Embryo Sac Development in the Maize *indeterminate gametophyte1* Mutant: Abnormal Nuclear Behavior and Defective Microtubule Organization

Bing-Quan Huang and William F. Sheridan[1]

Department of Biology, University of North Dakota, Grand Forks, North Dakota 58202-9019

The *indeterminate gametophyte1* mutation in maize has been known to disrupt development of the female gametophyte. Mutant embryo sacs have abnormal numbers and behavior of micropylar and central cell nuclei, which result in polyembryony and elevated ploidy levels in the endosperm of developing kernels. In this study, we confirm abnormal nuclear behavior and present novel findings. In contrast to the normal form, there is no obvious polarity in two-nucleate embryo sacs or in the micropylar cells of eight-nucleate embryo sacs. We show that the second and third mitoses are not fully synchronized and that additional mitoses can occur in all of the nuclei of the mutant embryo sac or in just the micropylar or central regions. After cellularization, individual micropylar cells can undergo mitosis. Abnormal microtubular behavior results in irregular positioning of the nuclei, asynchronous microtubular patterns in different pairs of nuclei, and abnormal phragmoplasts after the third mitotic division. These results indicate that in addition to acting primarily in controlling nuclear divisions, the *indeterminate gametophyte1* gene acts secondarily in regulating microtubule behavior. This cytoskeletal activity most likely controls the polarization and nuclear migration underlying the formation and fate of the cells of the normal embryo sac.

INTRODUCTION

In flowering plants, the polarity of the developing embryo sac is evident in the megasporocyte at early meiosis and is displayed along the micropylar–chalazal axis of the female gametophyte throughout its development. The polar distribution of the DNA-containing organelles is believed to be a key factor in the ultimate determination of cell fate during the selection of the functional megaspore and the formation of the seven-celled embryo sac (Willemse, 1981; Willemse and Van Went, 1984; Huang and Russell, 1992; Huang and Sheridan, 1994). During megagametogenesis, the micropylar and chalazal nuclei of the embryo sac undergo synchronized nuclear divisions and migration along the micropylar–chalazal axis at the second and third mitoses (Huang and Sheridan, 1994). This is followed by the simultaneous formation of cell walls, whereby the eight nuclei of the embryo sac are partitioned into seven cells (Haig, 1990; Huang and Russell, 1992; Bedinger and Russell, 1994). During embryo sac development, the microtubular cytoskeleton displays a number of distinct types of configurations and regular patterns (Webb and Gunning, 1990, 1994; Huang and Sheridan, 1994). It appears to function in the establishment and maintenance of organelle polarity and in the precise migration and positioning of the nuclei (Willemse and Van Lammeren, 1988; Huang et al., 1990; Webb and Gunning, 1990, 1994; Huang and Sheridan, 1994), thereby playing a fundamental role in cellular determination and differentiation of the normal embryo sac (Brown and Lemmon, 1991, 1992). These cytoskeletal functions are believed to be under genetic control (Staiger and Cande, 1990; Liu et al., 1993); however, little is known about their genetic regulation or the molecular mechanisms that may underlie this developmental process (Huang and Russell, 1992; Reiser and Fischer, 1993).

Only a few female gametophyte mutants have been reported (Singleton and Mangelsdorf, 1940; Nelson and Clary, 1952; Kermicle, 1969); among them, only the *indeterminate gametophyte1* (*ig1*) mutant has been subjected to cytological analysis (Lin, 1978, 1981). The *ig1* mutation of maize was first reported by Kermicle (1969) as a mutation conditioning the production of haploid embryos of paternal origin. This mutation, located on chromosome arm *3L*, results in an indeterminate number of micropylar cells and polar nuclei in the embryo sac (Lin, 1978, 1981). Consequently, it gives rise to polyembryony and variations in ploidy level of the endosperm after fertilization (Kermicle, 1969, 1971, 1994; Lin, 1984). This mutation affects not only the number of nuclear divisions in the embryo sac but also nuclear migration and cellular differentiation (Lin, 1978, 1981).

[1] To whom correspondence should be addressed.

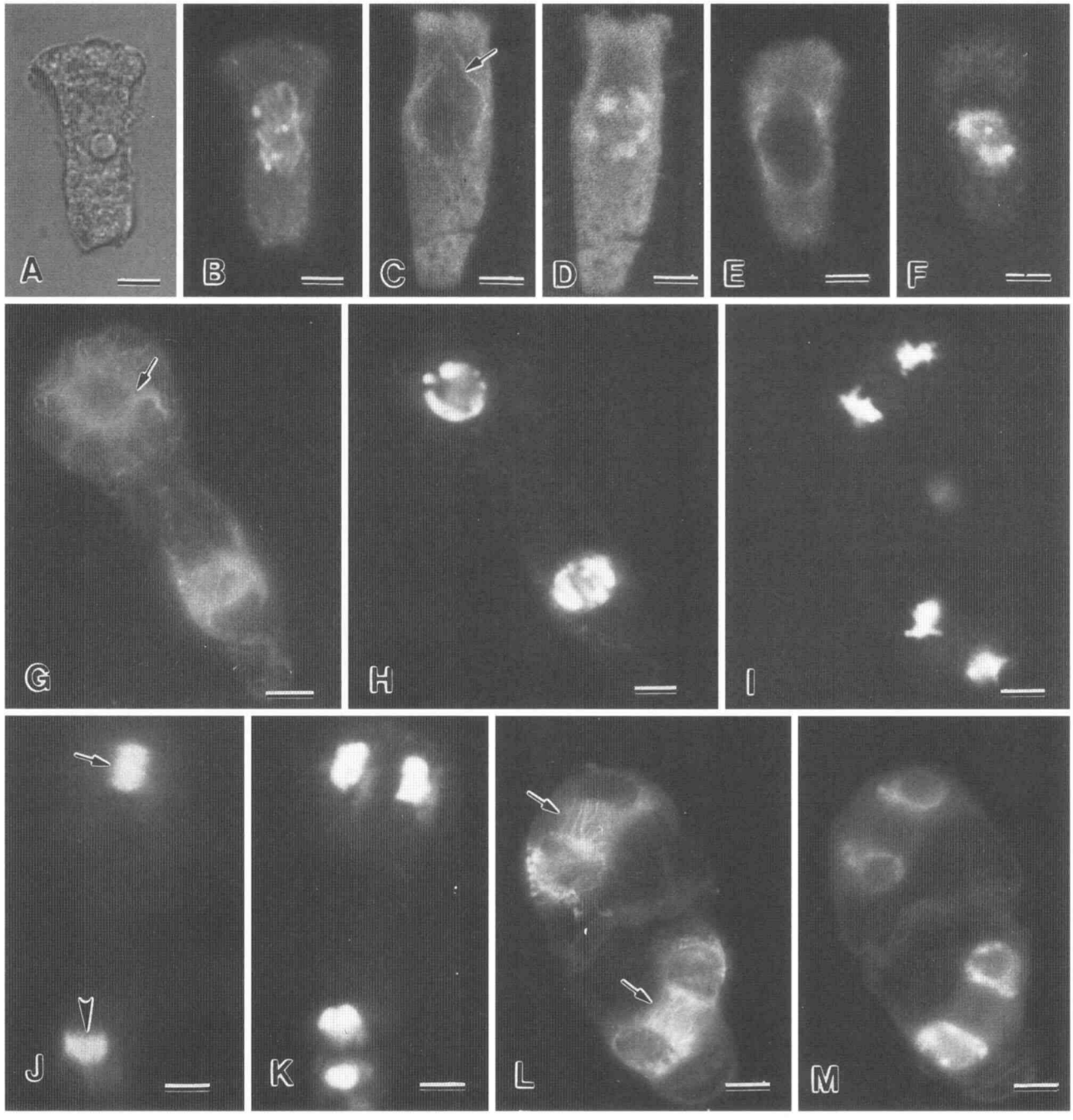

Figure 1. Organization of Microtubules and Nuclear DNA in a Normal Megasporocyte and Young Embryo Sac.

(A) An isolated megasporocyte at prophase I of meiosis.

(B) Chromosomes and organellar DNA of the cell shown in **(A)** stained with Hoechst 33258.

(C) Antitubulin antibody immunofluorescence staining of an isolated megasporocyte at anaphase I of meiosis, showing the perinuclear microtubules (arrow).

(D) Hoechst 33258 staining of the chromosomes in the cell shown in **(C)**.

(E) Perinuclear microtubules in the surviving megaspore.

(F) Nucleus of the megaspore shown in **(E)** stained with Hoechst 33258.

(G) Radiate perinuclear microtubules (arrow) connect the nucleus at the micropylar pole (upper) to the peripheral region of the two-nucleate embryo sac.

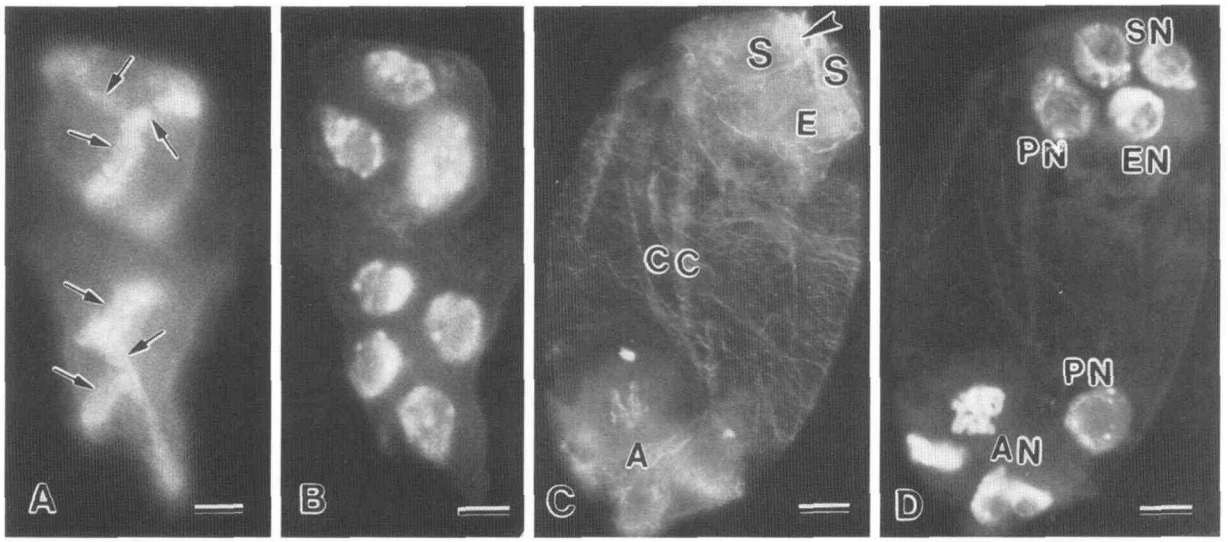

Figure 2. Organization of Microtubules and Nuclear DNA in Normal Embryo Sacs after Megagametogenesis.

(A) Simultaneous formation of phragmoplasts (arrows) after the third mitosis in both the micropylar and chalazal nuclei predicts the sites of future cell plate formation.

(B) Eight corresponding nuclei of the embryo sac shown in **(A)**.

(C) Organization of microtubules of the embryo sac after cellularization. Note the microtubule organization centerlike structure (arrowhead) at the site of the filiform apparatus. There are dense microtubule bundles in the synergid cells (S), transverse microtubules in the central cell (CC), and random microtubules in the antipodal cells (A). E, egg cell.

(D) Corresponding Hoechst 33258 staining of the eight-nucleate embryo sac shown in **(C)**. Two synergid nuclei (SN), one egg nucleus (EN), and one polar nucleus (PN) are located at the micropylar pole. Three antipodal cell nuclei (AN) and one polar nucleus are distributed at the chalazal pole of the embryo sac.

Bars in **(A)** to **(D)** = 2 μm.

In spite of the previous cytological studies of the *ig1* mutant, until now no information has been reported relating the abnormal pattern of nuclear migration and division with any corresponding cytoskeletal behavior and organization. The microtubular cytoskeleton is generally believed to play an important role in the determination of cell shape, in positioning and orientation of the organelles and nuclei, in organizing the mitotic spindle, and in the assembly of cell walls during cytokinesis (Derksen et al., 1990). The elucidation of cytoskeletal organization and modification during mutant embryo sac formation promises to be helpful in understanding the role of genes in the normal developmental process. In this study, we characterize nuclear behavior and changes to the organellar DNA and microtubular cytoskeleton during embryo sac development in both normal and *ig1* mutant stocks.

RESULTS

Nuclear Behavior and Microtubule Organization during Wild-Type Megasporogenesis and Megagametogenesis

At the beginning of megasporogenesis, the megasporocyte proceeds into prophase I of meiosis. At the pachytene stage, the nucleus, with a distinct nucleolus (Figure 1A), is located

Figure 1. (continued).

(H) Two nuclei at the two poles of the embryo sac shown in **(G)**.

(I) Embryo sac at telophase of the second mitotic division. Note the synchronous nuclear divisions of the second mitosis at the micropylar and chalazal poles.

(J) Another embryo sac after the second mitosis, with the phragmoplast microtubules aligned between the two pairs of sister nuclei. Note that the longitudinally aligned phragmoplast at the micropylar pole (arrow) is perpendicular to the transversely aligned phragmoplast at the chalazal pole of the embryo sac (arrowhead).

(K) Pairs of sister nuclei at the micropylar and chalazal poles after the second mitosis in the same embryo sac shown in **(J)**.

(L) Numerous microtubule bundles (arrows) are aligned between two pairs of nuclei of a four-nucleate embryo sac at a later stage.

(M) Four-nucleate embryo sac shown in **(L)**. Note that one of each pair of nuclei has migrated toward the center of the embryo sac.

Bars in **(A)** to **(M)** = 2 μm.

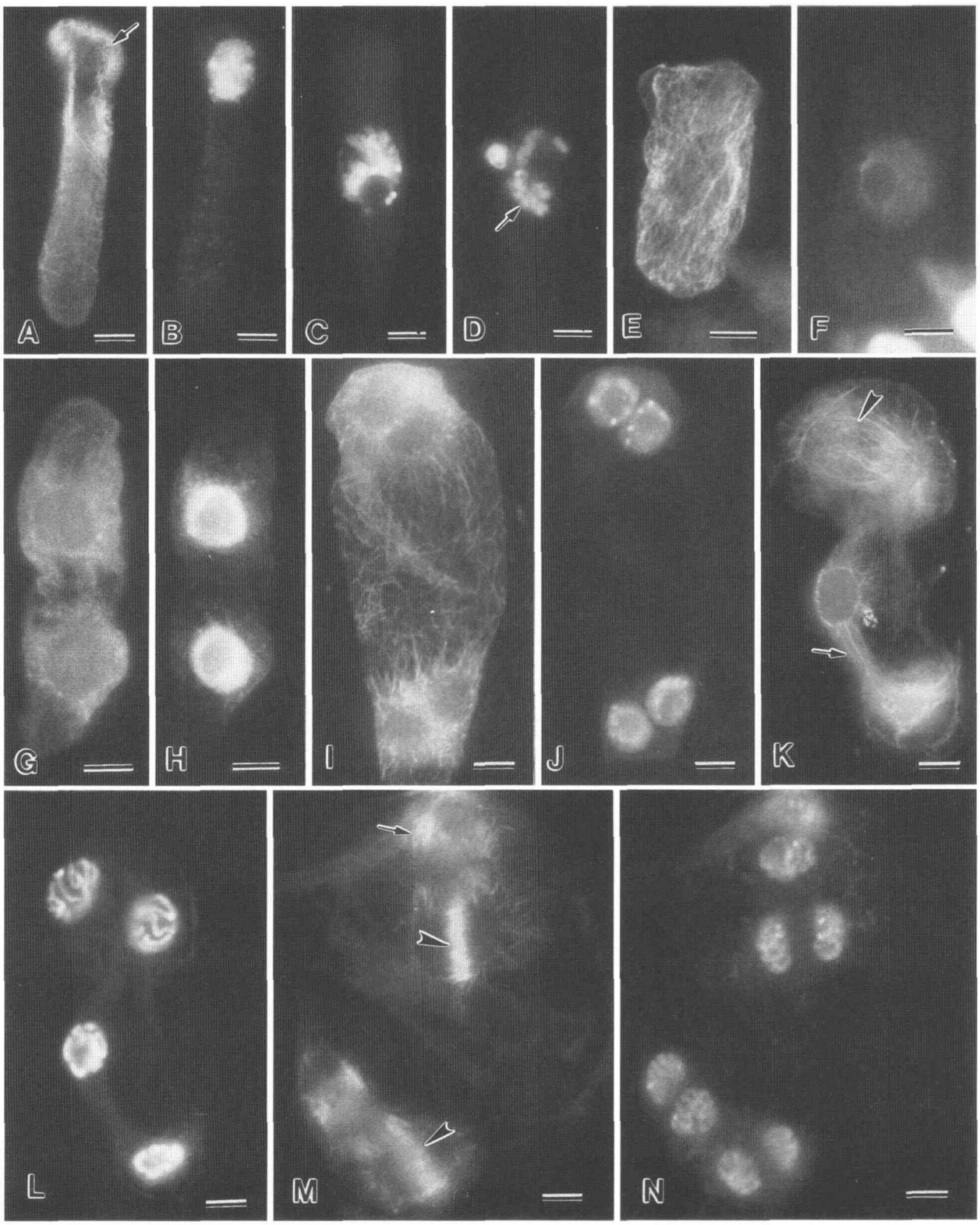

Figure 3. Organization of Microtubules and Organellar DNA in the *ig1* Mutant during Embryo Sac Development.

in the central region. The chromosomes and the chromosome knobs are distinguishable by staining with Hoechst 33258 (Figure 1B). During late prophase I of meiosis, the perinuclear microtublules become conspicuous and the chromosomes are readily visible in the cell (Figures 1C and 1D). After meiosis, the chalazal-most megaspore persists and comprises the initial cell of the female gametophyte generation. The microtubules are mostly perinuclear (Figure 1E), and the nucleus is located at the center of the cell (Figure 1F). The first mitotic division of the megaspore gives rise to the two-nucleate embryo sac, which undergoes considerable vacuolization during its elongation and enlargement. The width of the micropylar end of the embryo sac expands to a large extent. At this stage, the young embryo sac displays a conspicuous polarity because at the wider micropylar end, dense microtubule bundles extend from the perinuclear region out to the surrounding cortex of the embryo sac, whereas those in the chalazal end are present to a lesser extent (Figure 1G). Although it is not clearly evident in the figure, we regularly observed a greater abundance of organellar DNA in the micropylar region than in the chalazal region of the normal two-nucleate embryo (see Figure 4M in Huang and Sheridan, 1994).

Without any intervening wall formation, a second mitotic division occurs as synchronized mitotic divisions of both the micropylar and chalazal nuclei. Prophase of the second mitosis is distinguished by the simultaneous condensation of the chromosomes in the micropylar and chalazal nuclei (Figure 1H). During anaphase of the second mitosis, the separation of their daughter chromosomes occurs simultaneously at both ends of the embryo sac but in different directions. The daughter chromosomes in the micropylar region migrate in a nearly horizontal plane relative to the micropylar–chalazal axis, whereas those in the chalazal region move in a nearly longitudinal plane (Figure 1I). During the subsequent telophase stage, the two phragmoplasts simultaneously form between the sister nuclei at both poles of the embryo sac (Figure 1J) and, like the pairs of sister nuclei (Figure 1K), are oriented at nearly a right angle to each other. At a later stage of the four-nucleate embryo sac, one of each of the pairs of sister nuclei migrates synchronously away from its sister nucleus. They move, respectively, from the micropylar and chalazal poles, toward the center of the embryo sac. Numerous microtubule bundles are localized between the sister nuclei (Figure 1L), and the bundle ends obviously associate with the envelopes of the sister nuclei (Figure 1M).

At the third mitosis, the pairs of nuclei at the micropylar and chalazal poles all divide simultaneously. At cytokinesis, the phragmoplasts are organized synchronously at both the micropylar and chalazal poles, indicating the locations of the future cell plates between these nuclei. Three distinct phragmoplasts form between the sister and non-sister nuclei (Figures 2A and 2B). After formation of the cell walls, two synergids and the egg cell are located at the micropylar pole, three antipodal cells are located at the chalazal pole, and the central cell occupies the center of the embryo sac. At this stage, the two polar nuclei are still at opposite sides of the large vacuole that is located in the center of the central cell (Figure 2D). Numerous longitudinally aligned microtubule bundles are localized in the synergids, and sparse transverse microtubules are arrayed in the cortex of the central cell and randomly distributed in the antipodal cells (Figure 2C). The filiform apparatus forms, and the polar nuclei fuse immediately after the first division of the antipodal cells. The antipodal cells continue to divide and produce variable numbers of cells at the chalazal end. At the mature embryo sac stage, there are 40 or more antipodal cells (Randolph, 1936; Huang and Sheridan, 1994). In a normal

Figure 3. (continued).

(A) An isolated megaspore mother cell of the *ig1* mutant before meiosis. Note the dense reticular microtubules in the perinuclear region at the micropylar pole (arrow).
(B) Nucleus of the cell shown in **(A)** is localized at the micropylar-most region.
(C) Chromosomes of the *ig1* megasporocyte during early prophase I of meiosis.
(D) An isolated *ig1* megasporocyte stained with Hoechst 33258, showing the chromosomes (arrow) of late prophase I.
(E) Microtubules obliquely aligned to the longitudinal axis of the functional *ig1* megaspore.
(F) Nucleus of the megaspore shown in **(E)**.
(G) Perinuclear microtubules in the two-nucleate mutant embryo sac.
(H) Two nuclei in the embryo sac shown in **(G)** stained with Hoechst 33258.
(I) Radiate perinuclear microtubules surround the pairs of nuclei at both ends of a four-nucleate mutant embryo sac.
(J) Four-nucleate embryo sac shown in **(I)**, with the nuclei visualized by staining with Hoechst 33258.
(K) Asynchronous migration of the nuclei in a four-nucleate mutant embryo sac. Note the different patterns of microtubules between the pairs of the nuclei at the micropylar (arrowhead) and chalazal (arrow) poles.
(L) Micropylar and chalazal pairs of nuclei of the four-nucleate embryo sac shown in **(K)**. Note that the lower pair of nuclei has completed the entry into interphase, whereas the upper pair is still at the telophase stage.
(M) Asynchronous divisions occur at the third mitotic division, reflected by the different microtubular patterns at the pairs of nuclei. Note that radiate microtubules surround the micropylar-most pair of nuclei (arrow) and that the phragmoplasts are still visible between the sister nuclei at the central and chalazal region (arrowheads).
(N) Eight corresponding nuclei in the *ig1* embryo sac shown in **(M)**.
Bars in **(A)** to **(N)** = 2 μm.

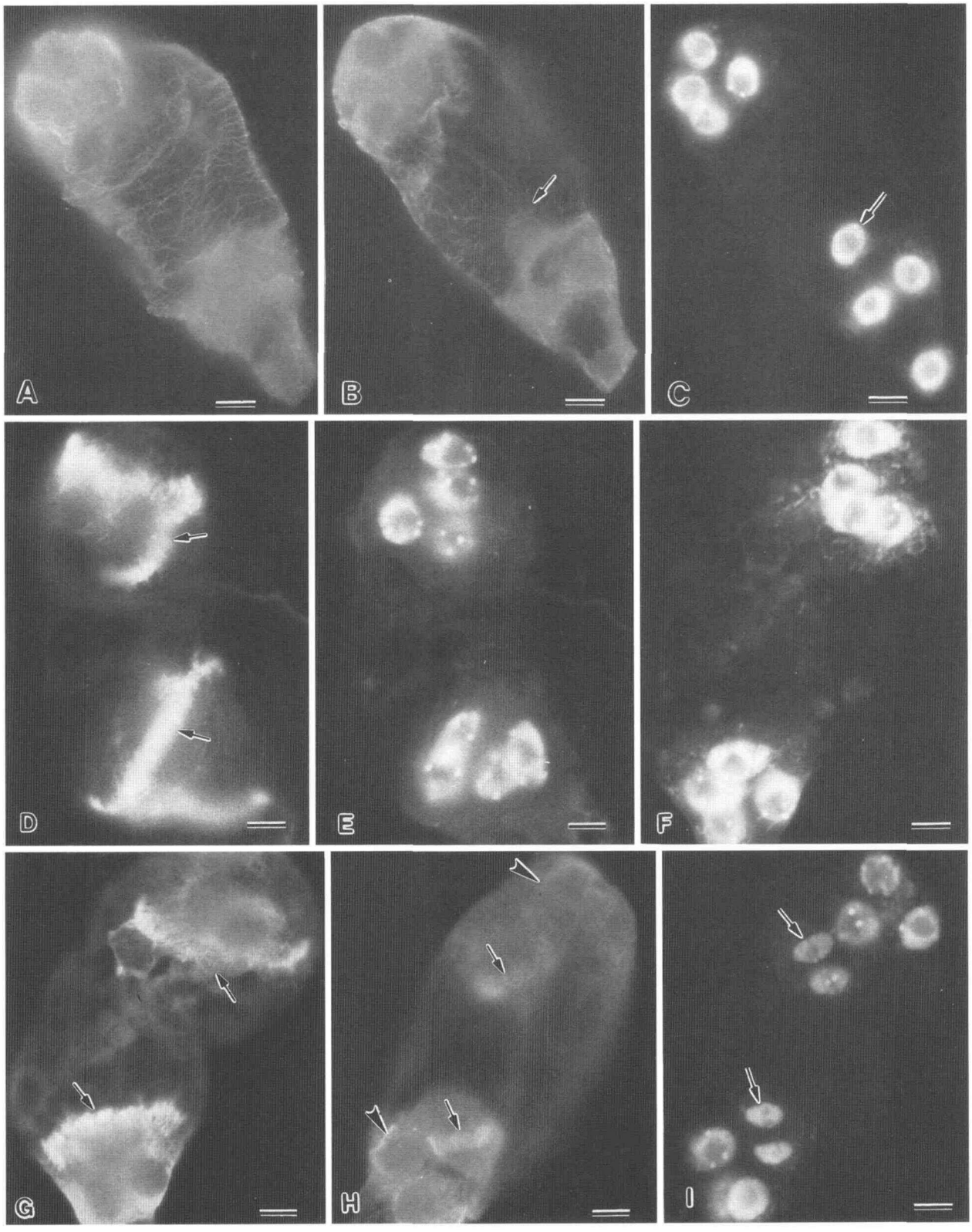

Figure 4. Variable Patterns of Microtubules and Nuclei in the *ig1* Embryo Sac after the Third Mitotic Division.

embryo sac, the antipodal cells are the only cells that undergo cell division before fertilization. In addition, the egg cell of the mature embryo sac normally contains abundant organellar DNA (see Figure 7F in Huang and Sheridan, 1994).

Nuclear Behavior and Microtubule Organization during Embryo Sac Development in the *ig1* Mutant

The *ig1* megasporocyte nucleus is located in the micropylar-most region. Dense perinuclear and cortical microtubules are localized predominantly at the micropylar pole of the cell (Figures 3A and 3B). At late prophase I, the chromosomes of the megasporocytes condense and are arranged in the center of the cell (Figures 3C and 3D). After meiosis, as in a normal stock, only the chalazal-most megaspore survives and becomes the functional megaspore that undergoes successive mitosis. Numerous oblique cytoplasmic microtubules are localized in the megaspore (Figure 3E), whereas its nucleus is located at the center of the cell (Figure 3F).

After the first mitotic division, both nuclei of the two-nucleate embryo sac are surrounded by dense perinuclear microtubules, but there is no obvious localization of organellar DNA at either the micropylar or the chalazal pole (Figures 3G and 3H). After the second mitotic division, one pair of sister nuclei is located at the micropylar pole, and a second pair is located at the chalazal pole, with numerous radiate microtubules present in the perinuclear region of each nucleus (Figures 3I and 3J). The second mitotic division is not fully synchronized, so at the late four-nucleate stage there occurs an asynchronized migration of one member of each pair of nuclei at both the micropylar and the chalazal poles. The pattern of microtubule bundles between sister nuclei as well as the positioning of the nuclei suggest that the migrating micropylar nucleus has moved to a lesser extent than has the migrating chalazal nucleus, which has numerous microtubules aligned between it and its sister nucleus (Figures 3K and 3L). The fact that micropylar nuclei both still are in the telophase stage, whereas both chalazal nuclei have already entered interphase (Figure 3L), confirms that the second mitotic division was not completely synchronized.

In contrast to the normal stock, the *ig* embryo sac displays a variety of abnormal patterns of microtubule and nuclear behavior during and after the third mitotic division. We have observed the following five abnormal patterns:

(1) Asynchronized division of the pairs of nuclei occurs at both the micropylar and chalazal poles. The different patterns of microtubules indicate that at the third mitosis, one nucleus at each pole completes its nuclear division ahead of the second nucleus at that pole. For example, when the micropylar-most nucleus has divided to produce daughter nuclei displaying radiate perinuclear microtubules, its sister nucleus has divided to produce daughter nuclei showing a longitudinally oriented phragmoplast (Figures 3M and 3N).

(2) Abnormal positioning of nuclei and phragmoplasts occurs in the third mitotic division. One nucleus of the group of four chalazal nuclei moves to the central region of the eight-nuclei embryo sac, whereas all four micropylar nuclei remain clustered at the micropylar pole (Figure 4C). The microtubules are perinuclear around both the micropylar- and the chalazal-clustered nuclei. Transverse microtubules are sparsely aligned in the cortex of the central region of the embryo sac (Figure 4A) but radiate out from the nucleus that has moved into the central region. The radiate microtubules connect this central-most chalazal nucleus to the cortex of the cell (Figure 4B). In some of the *ig1* embryo sacs, four nuclei and uniformly distributed organellar DNA are clustered in the micropylar pole, and another four nuclei are clustered in the chalazal pole. No nuclei were observed in the central region (Figures 4E and 4F). In some mutant embryo sacs of this type, an abnormal

Figure 4. (continued).

(A) Organization of microtubules in an eight-nucleate mutant embryo sac. Note the dense perinuclear microtubules in the micropylar nuclei (upper group) and the transverse microtubules in the periphery of the central region of the embryo sac.

(B) The same embryo sac shown in **(A)**, after adjusting the microscope to a deeper focus, showing the internal microtubule organization. Note the radiate microtubules connecting one of the chalazal nuclei (arrow) to the peripheral region of the embryo sac.

(C) The eight-nucleate embryo sac shown in **(A)** and **(B)** stained with Hoechst 33258. Note that one of the chalazal nuclei (arrow) has migrated toward the central region of the embryo sac.

(D) Abnormal phragmoplasts are visible (arrows) after the third mitosis in an *ig1* embryo sac. Note the irregular orientation and location of the phragmoplasts between the eight nuclei of the embryo sac. Compare this phragmoplast pattern with that of the normal embryo sac in Figure 2A.

(E) The same eight-nucleate *ig1* embryo sac shown in **(D)**. Note the four nuclei clustered at the micropylar pole and another four at the chalazal pole.

(F) An eight-nucleate *ig1* embryo sac. Note that four nuclei are clustered at the micropylar pole and another four are clustered at the chalazal pole in the embryo sac.

(G) Dense and compact microtubules surround the clustered micropylar and chalazal nuclei (arrows) shown in **(F)**.

(H) Another mutant embryo sac in which an additional nuclear division occurred in the two polar nuclei after the third mitotic division. Note the phragmoplast localized between each pair of sister nuclei in the central region (arrows); compact microtubules are visible at the perinuclear region of the rest of the micropylar and chalazal nuclei (arrowheads).

(I) Localization with Hoechst 33258 staining of the nuclei in the embryo sac shown in **(H)**. Note the two pairs of newly formed nuclei (arrows) in the central region.

Bars in **(A)** to **(I)** = 2 μm.

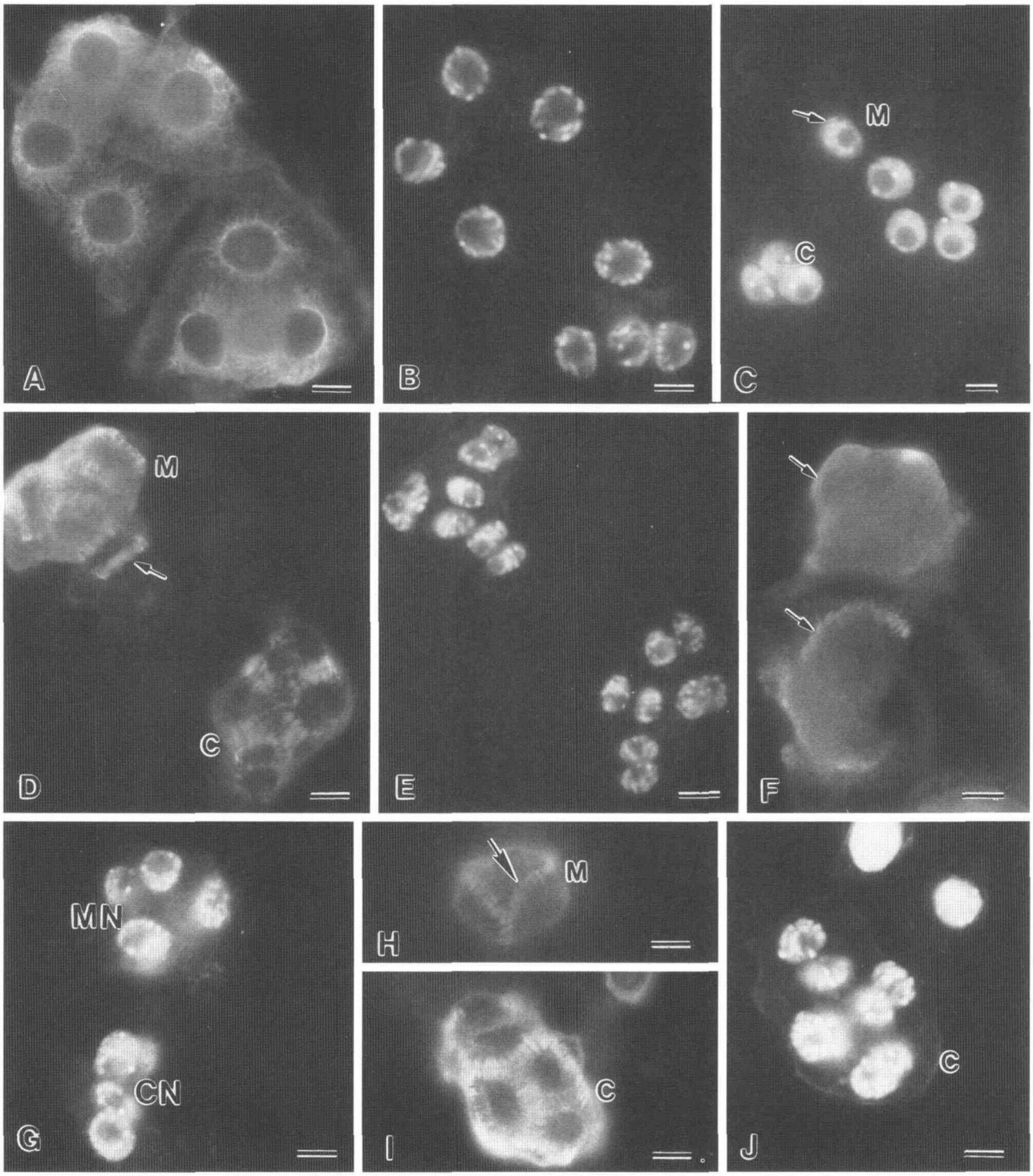

Figure 5. Organization of Microtubules and DNA in the *ig1* Mutant after Megagametogenesis.

(A) Radiate microtubules can be visualized at the perinuclear region of the eight free nuclei of the embryo sac.
(B) Localization of the eight nuclei in the embryo sac shown in **(A)**. Note the widespread dispersal of nuclei of the embryo sac.
(C) Abnormal nuclear pattern of another eight-nucleate embryo sac. Note the five nuclei located at the micropylar pole (M; arrow), whereas only three nuclei are distributed at the chalazal pole (C).

Table 1. Nuclear Distribution Pattern of Micropylar Nuclei in Mature Embryo Sacs of *ig1/ig1* Ovules

	Number of Micropylar Nuclei												
	1	2	3[a]	4	5	6	7	8	9	10	11	12	Total
Number of mature ovules[b]	1	0	34	3	21	23	29	3	4	2	0	2	122
Percentage of ovules	0.82	0	27.87	2.46	17.21	18.85	23.77	2.46	3.28	1.64	0	1.64	100

[a] Number of micropylar nuclei present in a normal embryo sac.
[b] Number of ovules containing an embryo sac with the corresponding number of micropylar nuclei.

organization of phragmoplasts occurs among the clustered nuclei at both the micropylar and chalazal poles (Figure 4D). After the third mitosis in other embryo sacs of this type, these clustered nuclei may be surrounded by dense short microtubule bundles at both the micropylar and chalazal poles (Figure 4G). Abnormal nuclear positioning was also observed, with five nuclei being distributed at the micropylar pole and three nuclei at the chalazal pole after the third mitosis (Figure 5C).

(3) An additional division occurs in the polar nuclei. After the third mitosis, the two polar nuclei undergo an additional mitosis, resulting in four polar nuclei (two pairs of sister nuclei) in the central region of the embryo sac (Figure 4I). The formation of a phragmoplast between the pairs of sister nuclei of each newly formed pair indicates the completion of this extra nuclear division. However, the microtubules in the micropylar and chalazal regions remain perinuclear (Figure 4H).

(4) Eight free nuclei are spread throughout the embryo sac after the third mitosis. The microtubules radiate from the nuclear envelopes of each of the eight nuclei (Figures 5A and 5B). This microtubular pattern is similar to that of maize endosperm nuclei at the free nuclear stage (B.-Q. Huang and W.F. Sheridan, unpublished data).

(5) A fourth mitosis occurs in all of the micropylar and chalazal nuclei. An additional fourth mitosis occurs simultaneously with each of the micropylar and chalazal nuclei, giving rise to a 16-nucleate embryo sac. A synchronized cytokinesis occurs following the fourth mitotic division. All of the phragmoplasts formed among the 16 nuclei at both the micropylar and chalazal poles are oriented in a ringlike pattern, except for the most central one, which is oriented transversely (Figures 5D and 5E). After the additional mitosis, the nuclei cluster in the micropylar, central, and chalazal regions in some of the *ig1* embryo sacs. Short and compact microtubules surround these clustered nuclei (Figure 5F), and ringlike phragmoplasts are localized between these nuclei (Figures 5F to 5H). Similar microtubular patterns are present in the chalazal region. The ringlike phragmoplasts (Figure 5I) are also found between these clustered chalazal nuclei (Figure 5J).

Variants and Ultrastructure of Indeterminate Gametophytes after Additional Mitoses

The asynchronized third and fourth mitotic divisions resulted in a variety of abnormal embryo sacs. The number of nuclei in the micropylar and central regions was variable. Table 1 shows that one to 12 nuclei were located at the micropylar pole and that slightly more than one-fourth of the *ig1* embryo sacs contained the normal three micropylar nuclei. Table 2 shows that one to eight nuclei were located in the central region and

Figure 5. (continued).

(D) Synchronous fourth mitotic divisions occur at both the micropylar and chalazal nuclei of another *ig1* embryo sac. Note the ringlike phragmoplasts organized between the nuclei at the micropylar (M) and chalazal (C) poles. A transverse phragmoplast (arrow) is aligned between the pair of the most centrally located sister nuclei of the micropylar group.

(E) Sixteen nuclei present in the embryo sac shown in **(D)**. Note that eight nuclei are located toward the micropylar pole (two of which are more centrally located), and another eight nuclei are located at the chalazal pole.

(F) Micropylar and central regions of a mutant embryo sac that underwent a fourth mitotic division. Compact microtubules (arrows) surround the groups of micropylar (MN) and central (CN) nuclei shown in **(G)**.

(G) Six nuclei (MN) are clustered in the micropylar pole (two of them are not in focus), and four nuclei (CN) are clustered in the central region of the same embryo sac shown in **(F)**.

(H) Antitubulin antibody staining of the micropylar region of the embryo sac shown in **(G)** reveals the phragmoplasts (arrow) located between the micropylar nuclei (M).

(I) Chalazal region (C) of the same embryo sac shown in **(F)** to **(H)**, with synchronized cytokinesis among the chalazal nuclei after the fourth mitotic division. Note the ringlike phragmoplasts organized between the nuclei.

(J) Eight nuclei are localized at the chalazal pole (C) of the embryo sac shown in **(I)**. Note that two central region nuclei are evident in the upper part of the figure.

Bars in **(A)** to **(J)** = 2 μm.

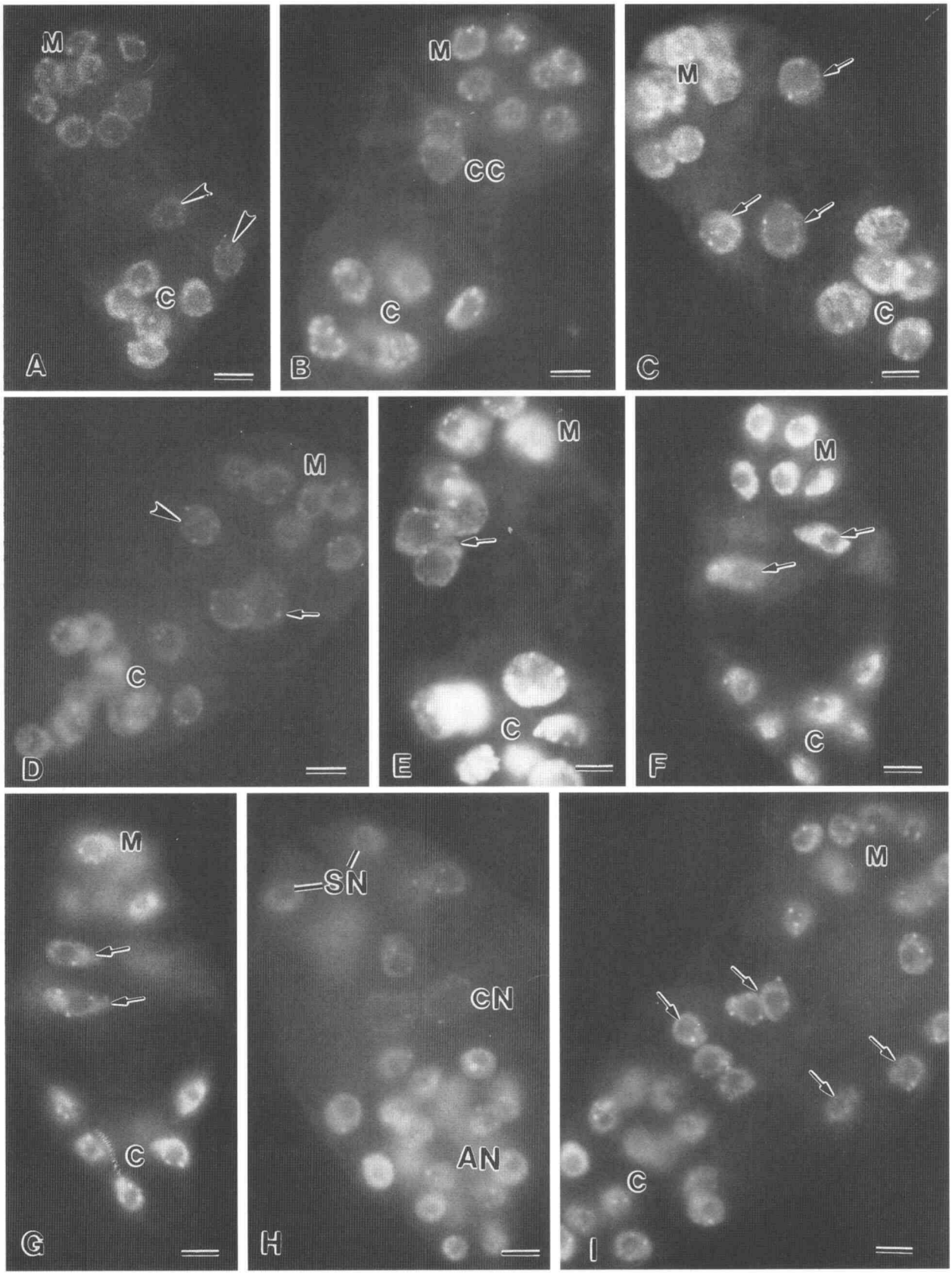

Figure 6. Abnormal Types of *ig1* Embryo Sacs.

Table 2. Nuclear Distribution Pattern of Polar Nuclei in Mature Embryo Sacs of *ig1/ig1* Ovules

	Number of Polar Nuclei								
	1	2[a]	3	4	5	6	7	8	Total
Number of mature ovules[b]	6	70	17	19	5	3	1	1	122
Percentage of ovules	4.92	57.38	13.93	15.57	4.10	2.46	0.82	0.82	100

[a] Number of polar nuclei present in a normal embryo sac.
[b] Number of ovules containing an embryo sac with the corresponding number of polar nuclei.

that slightly more than one-half of the *ig1* embryo sacs contained the normal two polar nuclei. Table 3 shows that ~25% of the *ig1/ig1* ovules had normal-appearing embryo sacs containing a total of five nuclei, with three at the micropylar region and two polar nuclei in the central region; the rest of the embryo sacs displayed some abnormality. Furthermore, ~72 and 43% of *ig1/ig1* ovules had an abnormal number of micropylar and central nuclei, respectively (Tables 1 and 2).

The abnormal embryo sacs differ not only in their number of nuclei but also in the size and distribution of their nuclei, as follows: (1) Two *ig1* embryo sacs had nine nuclei in the cluster at the micropylar pole and one nucleus in the central region (Figure 6A). (2) Sixteen embryo sacs had seven nuclei clustered at the micropylar pole and two polar nuclei in the central region, with the latter two often in the process of fusing together in the central region (Figure 6B). (3) One *ig1* embryo sac had

Table 3. Nuclear Distribution Pattern of Micropylar and Polar Nuclei in Mature Embryo Sacs of *ig1/ig1* Ovules[a]

	Number of Micropylar and Polar Nuclei														
	3	4	5[b]	6	7	8	9	10	11	12	13	14	16	>16	Total
Number of mature ovules[c]	1	1	31[d]	0	11	18	29	16	6	3	2	2	1	1	122
Percentage of ovules	0.82	0.82	25.41	0	9.02	14.75	23.77	13.11	4.92	2.46	1.64	1.64	0.82	0.82	100

[a] Data are shown for the number of micropylar and polar nuclei but not for the number of antipodal nuclei, because this number varies in normal mature embryo sacs.
[b] Number of micropylar and polar nuclei present in a normal embryo sac.
[c] Number of ovules containing an embryo sac with the corresponding number of micropylar and polar nuclei.
[d] All of these ovules contain embryo sacs with three micropylar and two polar nuclei; no embryo sacs were observed to have two micropylar and three polar nuclei.

Figure 6. (continued).

(A) A 16-nucleate *ig1* embryo sac. Note that nine nuclei are scattered at the micropylar pole (M), two nuclei (arrowheads) have migrated into the central region, and the remaining five nuclei are located at the chalazal pole (C).
(B) A different type of 16-nucleate *ig1* embryo sac. Note that seven nuclei are located at the micropylar pole (M) and at the chalazal pole (C); two polar nuclei appear to be fusing together in the central region (CC).
(C) A 16-nucleate *ig1* embryo sac. Note that there are eight nuclei at the micropylar pole (M), three dispersed nuclei in the center (arrows), and five nuclei at the chalazal pole (C).
(D) An isolated *ig1* embryo sac containing six nuclei at the micropylar pole (M), three nuclei in the center, and 12 nuclei at the chalazal pole (C). Note that the two centrally located adjacent nuclei fuse (arrow), whereas the third centrally located nucleus remains separate (arrowhead).
(E) Another 16-nucleate *ig1* embryo sac. Note that five nuclei (two are not in focus) are clustered at the micropylar pole (M), four nuclei are clustered in the central region (arrow), and the remaining seven nuclei are located at the chalazal pole (C).
(F) A 15-nucleate *ig1* embryo sac contains five nuclei in the micropylar pole (M), four in the center (arrows), and six in the chalazal pole (C). The two arrows point to two large central cell nuclei, and the other two central cell nuclei are not in focus (see **[G]**).
(G) A different focus of the embryo sac shown in **(F)**. The arrows point to the other two central cell nuclei.
(H) A 31-nucleate *ig1* embryo sac containing seven nuclei at the micropylar pole, two large central cell nuclei (CN), and 22 antipodal nuclei (AN). Note that the two nuclei occupying the micropylar-most region are appropriately located to become the synergid nuclei (SN).
(I) A 32-nucleate *ig1* embryo sac. Note that the central nuclei (arrows) do not differ in size from the micropylar (M) and chalazal (C) nuclei. Bars in **(A)** to **(I)** = 2 μm.

eight nuclei clustered at the micropylar pole and three scattered nuclei in the central region (Figure 6C). (4) Four *ig1* embryo sacs had six nuclei at the micropylar pole and three polar nuclei at the central region (Figure 6D). (5) Five *ig1* embryo sacs had five nuclei clustered at the micropylar pole and either four nuclei clustered in the central region (Figure 6E) or four scattered polar nuclei (Figures 6F and 6G). (6) In some of the *ig1* embryo sacs, two of the micropylar cells occupied the micropylar end, presumably becoming synergids with the other micropylar nuclei distributed in the micropylar region and with two polar nuclei appearing to approach each other in the central region (Figure 6H). (7) One *ig1* embryo sac had 19 uniform-appearing nuclei distributed throughout its micropylar and central regions (Figure 6I).

Electron microscopy of a normal embryo sac shows two synergid cells with a polarized distribution of cytoplasmic organelles (Figure 7A), whereas the ultrastructure of an *ig1* embryo sac reveals seven nonpolarized cells clustered at the micropylar pole (Figure 7B). Numerous vacuoles are evenly distributed throughout the mutant micropylar cells. Unlike the ultrastructure of the normal embryo sac, the mutant micropylar cells appear to have the same uniform cytoplasmic features. No obvious polarity of nuclei or cytoplasmic organelles is observed in these cells, and no specific cell types are identified. The mutant micropylar cells have fewer mitochondria and plastids when compared with normal cells, and these organelles are located mainly in the perinuclear region (Figure 8A) rather than being polarized at the micropylar end of cells, as is observed in the normal embryo sac (Figure 7A). Electron microscopic examination of *ig1* embryo sacs confirmed the occurrence of asynchronous nuclear divisions in these micropylar cells. One micropylar cell appears to be undergoing an extra mitosis, as indicated by the disappearance of the nuclear envelope and the presence of condensed chromosomes (Figure 8B).

DISCUSSION

Overview of the *ig1* Phenotype

Female gametophytes containing the *ig1* mutant allele are defective in several related aspects of their development, and this cascade of defects results in the formation of abnormal embryo sacs.

Abnormal Nuclear Behavior

The primary disturbance in mutant female gametophyte development is abnormal nuclear division behavior, as manifest by asynchronous nuclear divisions and their continuation among the micropylar and central cell nuclei beyond the usual eight-nucleate stage. In a normal embryo sac, excluding the three antipodal nuclei, there are five nuclei, with three nuclei occupying the two synergids and the egg cell and two comprising the polar nuclei of the central cell. Whereas in maize the antipodal cells continue to divide to form 40 or more cells, there are no further divisions of the micropylar or central cell nuclei before fertilization in a normal embryo sac. Instead of five nuclei in the central and micropylar regions, the number of nuclei in these regions can reach as many as 14 in a given *ig1* embryo sac, and the ploidy of developing endosperms can range from two sets (2X) to nine sets (9X) of chromosomes, according to Lin (1981). We confirm and extend these observations on the abnormal number and arrangement of nuclei. At the micropylar end, we observe five or more nuclei; in the central region, the number of nuclei ranges from one to several. It is evident that loss of normal control of nuclear behavior results both in abnormal division and in the placement of nuclei in abnormal locations. Abnormal positioning of nuclei during embryo sac development appears to result from defects in nuclear migration. In some mutant embryo sacs, nuclei in the central region apparently fuse, resulting in larger than normal nuclei. The highly orchestrated and synchronized nuclear movements that normally occur during the second and third mitotic divisions are lacking.

Abnormal Behavior of the Tubulin Cytoskeleton

Abnormal microtubule patterns accompany the unsynchronized and abnormal nuclear movements. Crucial features of normal embryo sac development include the intersister nuclei microtubules and the display of each mitotic apparatus in precise orientation between pairs of nuclei at both poles of the embryo sac, with perpendicular orientation between the spindles separating the non-sister nuclei. Both of these features appear to be important in the precise positioning of nuclei during the second and third mitoses (Huang and Sheridan, 1994). However, these features are lacking during the second and third mitoses in mutant embryo sacs. Phragmoplast formation is also abnormal in mutant embryo sacs. Instead of the simultaneous formation of phragmoplasts between the nuclei at the micropylar and chalazal poles, the *ig1* embryo sacs exhibit irregular phragmoplasts that are either centrifugally organized between the clustered nuclei or irregularly aligned among the eight nuclei distributed between the micropylar and chalazal poles of the embryo sac. Furthermore, some of the *ig1* embryo sacs display radiate perinuclear microtubules at the eight-nucleate stage that are analogous to the prophase microtubule pattern of endosperm (Van Lammeren, 1988; Brown et al., 1994).

Lack of Specialization of Micropylar Cells

As a consequence of both the asynchronous nuclear divisions, with some or all of the nuclei of the micropylar and central regions undergoing additional divisions, and the abnormal nuclear migration, the nuclei in the micropylar and central regions

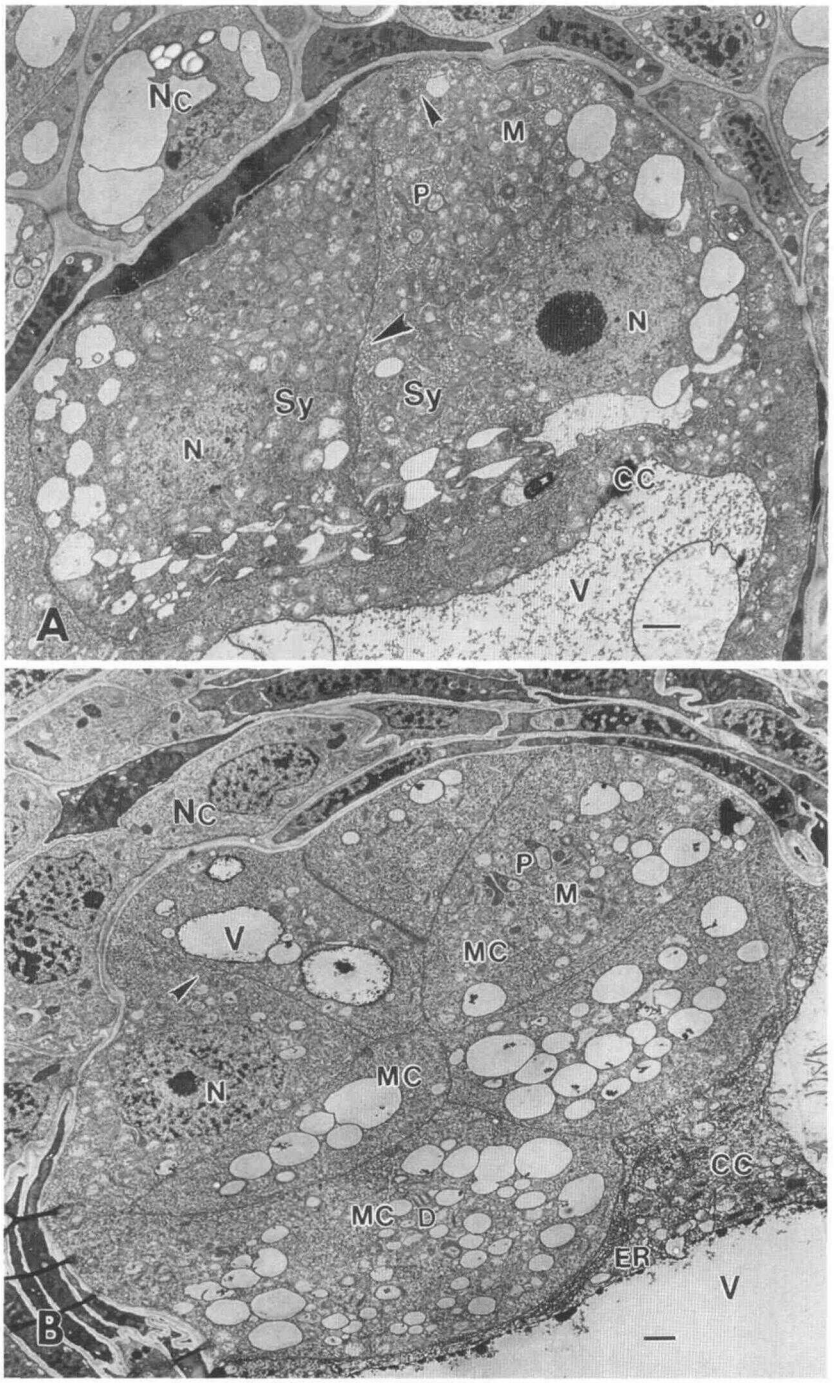

Figure 7. Ultrastructure of the Normal and *ig1* Embryo Sacs.

(A) Nucellus (Nc) enclosing a normal embryo sac with two synergid cells (Sy) occupying its micropylar end. Note that numerous plastids (P), mitochondria (M), and vacuoles are located at the micropylar pole. Abundant endoplasmic reticulum is distributed at the cortex of the cell (arrowheads). The synergid nuclei (N) are located toward the chalazal end of both cells. A large vacuole (V) occupies much of the central cell (CC). **(B)** An *ig1* embryo sac with seven micropylar cells (MC) having the same cellular appearance. Numerous vacuoles (V) are distributed throughout the cells. Abundant endoplasmic reticulum (arrowhead) is present at the cortex of the micropylar cells. There are no distinguishable cell types among the micropylar cells. There is a large vacuole in the central cell (CC). D, dictysome; ER, endoplasmic reticulum; M, mitochondria; N, nucleus; Nc, nucellus; P, plastids.

Bars in **(A)** and **(B)** = 0.5 μm.

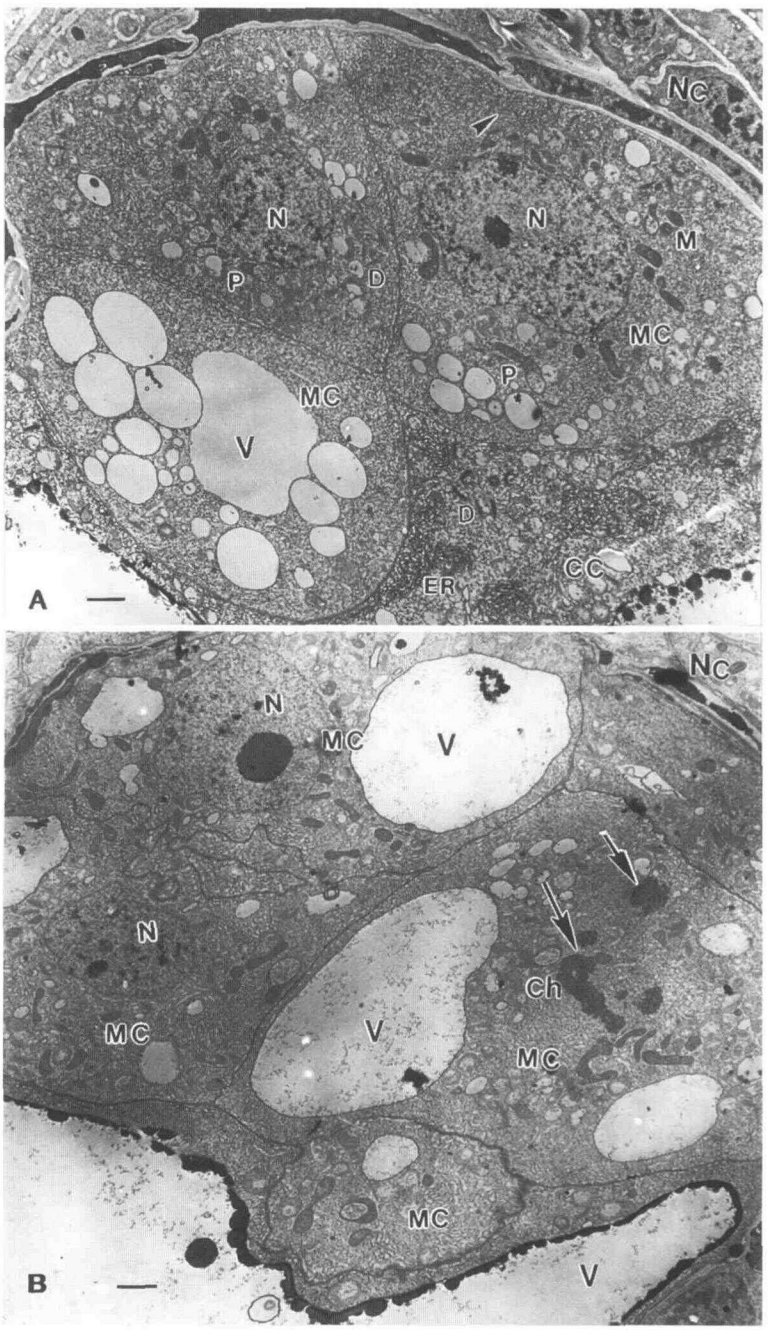

Figure 8. Cellular Organization in the Micropylar Region of the *ig1* Embryo Sac and Asynchronous Nuclear Divisions among the Micropylar Cells.

(A) Another *ig1* embryo sac in which the micropylar cells (MC) display no obvious polarity. Note that fewer plastids (P) and mitochondria (M) are present in these cells compared with those of the normal embryo sac. These cytoplasmic organelles surround the nuclei (N), which are located in the center of the cells. Numerous vacuoles (V) are distributed throughout the cells. Abundant endoplasmic reticulum is located in the cortex of the cells (arrowhead). Some dictysomes are distributed in the cytoplasm of the micropylar cells. Abundant endoplasmic reticulum (ER) and dictysomes are located in the cortex of the central cell (CC). D, dictysome; Nc, nucellus cell.

(B) Asynchronous nuclear divisions after cellularization in an *ig1* embryo sac. Condensed chromosomes (arrows) indicate that one of the micropylar cells is in the mitotic anaphase stage; the rest of the cells are in the interphase stage. Ch, chromosome; MC, micropylar cell; N, nucleus; Nc, nucellus cell; V, vacuole.

Bars in **(A)** and **(B)** = 0.5 μm.

of the *ig1* embryo sac are indeterminate in number and positioning. When cellularization occurs during the terminal stage of mutant embryo sac development, the micropylar cells of the *ig1* embryo sac display such a strong ultrastructural similarity that the synergid and egg cells are indistinguishable. In approximately two-thirds (69%) of the *ig1* embryo sacs, five or more such cells occupy the micropylar region, and based on our ultrastructural examination of 10 such embryo sacs, they are all likely to be identical in ultrastructural appearance. It is intriguing that although some of them function as synergid cells, they lack two structural features characteristic of synergids: none of them displays either the polarized distribution of vacuoles at their chalazal-most region or the "filiform apparatus" at their micropylar end, which frequently has been imputed to attract pollen tubes into the female gametophyte (Huang and Russell, 1992, 1994; Huang et al., 1993).

Abnormal Migration and Positioning of Nuclei

We believe that the apparent lack of cellular specialization of micropylar cells of *ig1* embryo sacs results from the abnormal migration and positioning of nuclei in the micropylar region. According to Brown and Lemmon (1991, 1992), "cytoplasmic domains" may determine the fate of cells during cell partitioning. The apparent lack of normal organellar DNA localization in the micropylar region may contribute to the lack of obvious cellular specialization. Even though our ultrastructural analysis indicated that all five or more micropylar cells appear the same, our light microscopic analysis of whole-mount mutant embryo sacs examined about the time of fertilization indicated that only some of the micropylar cells are functional. Among the several cells in the micropylar region, the micropylar-most cells appear to function frequently as synergids for receipt of pollen tubes and male gametes (B.-Q. Huang and W.F. Sheridan, unpublished data). One or more of the other micropylar cells may function as eggs, resulting in up to 6% polyembryony (Kermicle, 1971). None or up to five of these micropylar cell were found by Lin (1978) to function as eggs in the *ig1* embryo sac, and it is likely that most of these micropylar cells have the potential to function as egg cells during fertilization. It is noteworthy that although these micropylar cells lack the usual polarity and structural features that distinguish synergids from egg cells, they apparently function as either cell type. This agrees with the suggestion that through a dedifferentiation process, plant cells seem to acquire a competence to be switched into sporophytic and gametophytic development (Dickinson, 1994; Sheridan et al., 1996).

Primary Defect and Secondary Effects in the *ig1* Mutation

We believe that the primary defect in the *ig1* mutation is in the regulation of the nuclear division cycle in the female gametophyte. This defect results in a loss of control in both the timing and extent of nuclear divisions. Because the third (and subsequent) divisions can occur asynchronously and all or some of the nuclei of an *ig1* embryo sac can continue to divide beyond the third mitotic division, the regulation of the third division is a crucial process requiring normal *ig1* activity. It appears that the nuclei fail to receive a signal that may both synchronize their third division and mark it as the terminal division for those nuclei that will occupy the micropylar and central regions.

It is likely that abnormal microtubular behavior during and following the third nuclear division is a secondary effect of the defect in regulation of the nuclear division cycle. The nuclei apparently fail to engage in their normal synchronized interactions with components of the microtubular cytoskeleton such that the usual pattern of nuclear migration and the resulting nuclear positioning, as well as the usual pattern of synchronized phragmoplast formation, are disrupted. These abnormalities, together with the continued division of one or more nuclei, can result in the presence of more than two nuclei in the central cell and more than three micropylar cells, and in the failure of the latter to differentiate their usual cellular specializations. Therefore, it appears likely that the variations in number of central cell (polar) nuclei (that result in abnormal and often defective endosperm development) and in number and indeterminate fate of micropylar cells are all indirect results of the primary defect in the regulation of the nuclear division cycle. The normal *ig1* gene product may function in the control point that switches off further nuclear divisions. Failure of this switching action may result in the failure of changes in those features of the nuclear envelope that may be required for proper interaction with microtubules and for proper nuclear migration.

Other Pleiotropic Effects Are Likely to Be Downstream of the Defect in Nuclear Behavior

The pleiotropic effects of the *ig1* mutation include abnormalities in cytoskeletal behavior, nuclear migration, and cellular differentiation, in addition to its effects on nuclear divisions (Lin, 1978, 1981; this report). This pleiotropy is consistent with the suggestion by Lin (1981) that the *ig1* locus does not control a single process but regulates the activity of other genes. Therefore, when the normal allele "mutates to *ig*, the entire functional pattern of these genes is out of control" (Lin 1981).

A similar multiplicity of effects encompassing both cytoskeletal organization and meiotic chromosome behavior has also been observed in certain meiotic mutants of maize. All of these defects are believed to stem from abnormal numbers of microtubules and/or a change in microtubule dynamics (Liu et al., 1993; Staiger and Cande, 1990). However, we believe it is likely that normal development of the microtubular cytoskeleton and its role during embryo sac formation depend on the prior proper regulation of the nuclear division process, including synchronous formation of daughter nuclei and nuclear envelopes that can interact correctly with the microtubules. Beyond the

abnormal behavior of the nuclei, we believe that the pleiotropic effects of the *ig1* mutation are the downstream effects of the defect in regulation of nuclear behavior.

METHODS

Plant Material

The source of immature ears was maize plants grown from kernels kindly provided by J.L. Kermicle (University of Wisconsin, Madison). The seed were produced by crossing the inbred M14 homozygous for *ig1* with pollen from the inbred A158 also homozygous for *ig1*. The plants were grown in a greenhouse lighted for 16 hr. Young ears were collected at the stage of tassel emergence, and the ovule developmental stages were estimated according to the length of the silk (Huang and Sheridan, 1994).

Double Labeling of Microtubules and DNA

Ovules were dissected and fixed in a mixture consisting of 4% paraformaldehyde, 10% DMSO, 0.1% Triton X-100 in PEMG buffer (50 mM Pipes, 2 mM $MgSO_4$, 5 mM EGTA, and 4% glycerol, pH 6.8) for 30 to 40 min at room temperature. After rinsing with PEMG buffer three to four times, we incubated materials in an enzyme solution (2% cellulysin, 2% pectinase, 0.3% pectolyase, and protease inhibitor in PEMG buffer) at 37°C for 1 hr. The protease inhibitor consisted of 2 mM phenylmethylsulfonyl fluoride, 16 μM leupeptin, and 25 μM pepstatin. The isolation of embryo sacs and double labeling of DNA and microtubules followed the procedure described by Huang and Sheridan (1994). Light microscopy was conducted using a microscope (Laborlux, S., Leitz, Germany) equipped for differential interference contrast and epifuorescence microscopy.

Transmission Electron Microscopy

The ear florets, including the ovules, were dissected from the ears from both the wild-type plants (+/+) and mutants (*ig1/ig1*) and fixed in a solution of 3% glutaraldehyde in 0.1 M sodium cacodylate buffer, pH 7.2, for 5 min under vacuum and further fixed in glutaraldehyde for 4 hr at room temperature. Materials then were postfixed for 12 hr in buffered 1% osmium tetroxide at 4°C, dehydrated in an ethanol series followed by propylene oxide, and embedded in Spurr's low viscosity resin. Longitudinal sections of ovules were cut at 70 to 80 nm by using a diamond knife and collected on Formvar-coated carbon-stabilized slotted grids (1 × 2 mm; Polysciences, Inc., Warrington, PA). Sections were stained with uranyl acetate for 30 min and then in Sato's lead citrate, as modified by Hanaichi et al. (1986). The sections were observed using an electron microscope (JEM-100 S; JEOL Ltd, Tokyo, Japan) operating at 80 KV.

ACKNOWLEDGMENTS

We thank Jerry Kermicle for the gift of seed used in this project. We also thank him and Jan Clark for their critical reading of the manuscript. The research was supported by U.S. Department of Agriculture Grant No. 94-37304-1045.

Received April 1, 1996; accepted June 5, 1996.

REFERENCES

Bedinger, P., and Russell, S.D. (1994). Gametogenesis in maize. In The Maize Handbook, M. Freeling and V. Walbot, eds (New York: Springer-Verlag), pp. 48–61.

Brown, R.C., and Lemmon, B.E. (1991). The cytokinetic apparatus in meiosis: Control of division plane in the absence of a preprophase band of microtubules. In The Cytoskeletal Basis of Plant Growth and Form, C.W. Lloyd, ed (New York: Academic Press), pp. 259–273.

Brown, R.C., and Lemmon, B.E. (1992). Cytoplasmic domain: A model for spatial control of cytokinesis in reproductive cells of plants. Electron Microsc. Soc. Am. Bull. **22,** 48–53.

Brown, R.C., Lemmon, B.E., and Olsen, O.-A. (1994). Endosperm development in barley: Microtube involvement in the morphogenetic pathway. Plant Cell **6,** 1241–1253.

Derksen, J., Wilms, F.H.A., and Pierson, E.S. (1990). The plant cytoskeleton: Its significance in plant development. Acta Bot. Neerl. **39,** 1–18.

Dickinson, H.G. (1994). The regulation of alternation of generation in flowering plants. Biol. Rev. **69,** 419–442.

Haig, D. (1990). New perspectives on the angiosperm female gametophyte. Bot. Rev. **56,** 236–274.

Hanaichi, T., Sato, T., Iwamoto, T., Malavasi, J., Hoshina, M., and Mizuno, N. (1986). A stable lead by modification of Sato's method. J. Electron Microsc. **35,** 304–306.

Huang, B.-Q., and Russell, S.D. (1992). Female germ unit: Organization, isolation and function. Int. Rev. Cytol. **140,** 233–293.

Huang, B.-Q., and Russell, S.D. (1994). Fertilization in *Nicotiana tabacum*: Cytoskeletal modification during synergid degeneration: An hypothesis for short distance transport of sperm cells prior to gamete fusion. Planta **194,** 200–214.

Huang, B.-Q., and Sheridan, W.F. (1994). Female gametophyte development in maize: Microtubular organization and embryo sac polarity. Plant Cell **6,** 845–861.

Huang, B.-Q., Russell, S.D., Strout, G.W., and Mao, L.J. (1990). Organization and characteristics of isolated embryo sac and egg of *Plumbago zeylanica*. Am. J. Bot. **11,** 1401–1410.

Huang, B.-Q., Pierson, E.S., Russell, S.D., Tiezzi, A., and Cresti, M. (1993). Cytoskeletal organization and modification during pollen tube arrival, gamete delivery and fertilization in *Plumbago zeylanica*. Zygote **1,** 143–154.

Kermicle, J.L. (1969). Androgenesis conditioned by a mutation in maize. Science **116,** 1422–1424.

Kermicle, J.L. (1971). Pleiotropic effects on seed development of the *indeterminate gametophyte* gene in maize. Am. J. Bot. **58,** 1–7.

Kermicle, J.L. (1994). *Indeterminate gametophyte (ig)*: Biology and use. In The Maize Handbook, M. Freeling and V. Walbot, eds (New York: Springer-Verlag), pp. 388–393.

Lin, B.-Y. (1978). Structural modifications of the female gametophyte associated with the *indeterminate gametophyte* (*ig1*) mutant in maize. Can. J. Cytol. **20,** 249–257.

Lin, B.-Y. (1981). Megagametogenetic alternations associated with the *indeterminate gametophyte* (*ig1*) mutant in maize. Rev. Bras. Biol. **41,** 557–563.

Lin, B.-Y. (1984). Ploidy barrier to endosperm development in maize. Genetics **107,** 103–115.

Liu, Q., Golubovskaya, I., and Cande, W.Z. (1993). Abnormal mutant alleles of *polymitotic* that disrupt the cell cycle progression from meiosis to mitosis in maize. J. Cell Sci. **106,** 1169–1178.

Nelson, O.E., and Clary, G.R. (1952). Genic control of semi-sterility in maize. J. Hered. **43,** 205–210.

Randolph, L.F. (1936). Developmental morphology of the caryopsis in maize. J. Agric. Res. **53,** 881–916.

Reiser, L., and Fischer, R.L. (1993). The ovule and the embryo sac. Plant Cell **5,** 1291–1301.

Sheridan, W.F., Avalkina, N.A., Shamrov, I.I., Batygina, T.B., and Golubovskaya, I.N. (1996). The *mac1* gene: Controlling the commitment to the meiotic pathway in maize. Genetics **142,** 1009–1020.

Singleton, W.R., and Mangelsdorf, P.C. (1940). Gametic lethals on the fourth chromosome of maize. Genetics **25,** 366–390.

Staiger, C.J., and Cande, W.Z. (1990). Microtubule distribution in *dv*, a maize meiotic mutant defective in the prophase to metaphase transition. Dev. Biol. **138,** 231–242.

Van Lammeren, A.A.M. (1988). Structure and function of the microtubular cytoskeleton during endosperm development in wheat: An immunofluorescence study. Protoplasma **146,** 18–27.

Webb, M.C., and Gunning, B.E.S. (1990). Embryo sac development in *Arabidopsis thaliana*. I. Megasporogenesis, including the microtubular cytoskeleton. Sex. Plant Repro. **3,** 244–256.

Webb, M.C., and Gunning, B.E.S. (1994). Embryo sac development in *Arabidopsis thaliana*. II. The cytoskeleton during megagametogenesis. Sex. Plant Repro. **7,** 153–163.

Willemse, M.T.M. (1981). Polarity during megasporogenesis and megagametogenesis. Phytomorphology **31,** 124–134.

Willemse, M.T.M., and Van Lammeren, A.A.M. (1988). Structure and function of the microtubular cytoskeleton during megasporogenesis and embryo sac development in *Gasteria verrucosa* (Mill.) H. Duval. Sex. Plant Repro. **1,** 74–82.

Willemse, M.T.M., and Van Went, J.L. (1984). The female gametophyte. In Embryology of Angiosperms, B.M. Johri, ed (New York: Springer-Verlag), pp. 159–196.